Adıyaman University Journal of Science
https://dergipark.org.tr/en/pub/adyujsci
DergiPark AKADEMİK
ISSN 2147-1630
e-ISSN 2146-586X

Effect of Nano-Sized Eu Substituting on Mechanical Properties of $Bi_{1.7}Pb_{0.3}Sr_2Ca_2Cu_{2.75}Na_{0.25}O_y$ Ceramic Superconductor System

Mehmet Ersin AYTEKİN[1,*], Mustafa AKYOL[2]

[1]*Tarsus University, Vocational School of Technical Sciences at Mersin Tarsus Organized Industrial Zone, Department of Electronics and Automation, 33100, Mersin, Türkiye*
mehmetaytekin@tarsus.edu.tr, ORCID: 0000-0003-0731-2034
[2]*Adana Alparslan Türkeş Science and Technology University, Faculty of Engineering, Department of Materials Science and Engineering, 01250, Adana, Türkiye*
makyol@atu.edu.tr, ORCID: 0000-0001-8584-0620

Received: 30.05.2025 **Accepted:** 05.12.2025 **Published:** 31.12.2025

Abstract

In this paper, the morphological, structure and mechanical properties of the superconducting system $Bi_{1.7}Pb_{0.3}Sr_{2-x}(Eu)_xCa_2Cu_{2.75}Na_{0.25}O_y$ (x = 0.00, 0.20, 0.25 and 0.30) have been investigated. Phase formation, morphological structure and mechanical properties of nano-sized Eu (80 nm) substituted ceramic samples prepared by solid state reaction method were characterized by X-ray Diffraction (XRD), Scanning Electron Microscopy (SEM) and Vickers microhardness instrument, respectively. Bi, Pb-2223 high temperature phases, Bi-2212 low temperature superconductor phase, and minor impurity phase production were identified in the X-ray measurement data. In all samples, the main phase structure is the tetragonal symmetric Bi-2223 superconducting phase. According to the SEM examination findings, the Bi-2223 phase has been detected by flaky plate-like grain types. With a uniform distribution of grains and strong connections between them, the sample containing Eu at the nano-sized ratio of x = 0.25 has a less porous morphological structure. Because strong intergranular bonds and a decreased void

* Corresponding Author DOI: 10.37094/adyujsci.1707341

structure were formed, the sample with nano-sized Eu substitution at x = 0.25 exhibited the best mechanical properties, according to the results of the microhardness measurement.

Keywords: Bi,Pb-2223; Microhardness; Meyer's law; Vickers; $Bi_{1.7}Pb_{0.3}Sr_{2-x}(Eu)_xCa_2Cu_{2.75}Na_{0.25}O_y$; SEM.

$Bi_{1.7}Pb_{0.3}Sr_2Ca_2Cu_{2.75}Na_{0.25}O_y$ Seramik Süperiletken Sisteminde Mekaniksel Özellikleri Üzerine Nano-Boyutlu Eu Katkısının Etkisi

Öz

Bu çalışmada, $Bi_{1.7}Pb_{0.3}Sr_{2-x}(Eu)_xCa_2Cu_{2.75}Na_{0.25}O_y$ (x = 0.00, 0.20, 0.25 ve 0.30) süperiletken sisteminin morfolojik yapısı ve mekanik özellikleri incelenmiştir. Katı hal tepkime yöntemi ile hazırlanan nano boyutlu Eu (80 nm) katkılı seramik örneklerin faz oluşumu, morfolojik yapısı ve mekanik özellikleri sırasıyla X-ışını Kırınımı (XRD), Taramalı Elektron Mikroskobu (SEM) ve Vickers mikrosertlik cihazı ile karakterize edilmiştir. X-ışını ölçüm verilerinde Bi, Pb-2223 yüksek sıcaklık fazları, Bi-2212 düşük sıcaklık süperiletken fazı ve minör safsızlık fazı üretimi tespit edildi. Tetragonal simetriye sahip Bi-2223 süperiletken fazı, tüm numunelerde temel faz yapısıdır. SEM inceleme bulgularına göre, plaka benzeri tane tiplerinde Bi-2223 fazı tespit edilmiştir. Taneciklerin düzgün dağılımı ve aralarında güçlü bağlantılar ile x = 0.25 nano boyutlu oranda Eu içeren örnek daha az gözenekli bir morfolojik yapıya sahiptir. Güçlü tanecikler arası bağlar ve az boşluklu yapı oluştuğu için, x = 0.25'te nano boyutlu Eu katkısı olan örnek, mikro sertlik ölçümünün sonuçlarına göre en iyi mekanik özellikleri sergilemiştir.

Anahtar Kelimeler: Bi,Pb-2223; Microhardness; Meyer's yasası; Vickers; $Bi_{1.7}Pb_{0.3}Sr_{2-x}(Eu)_xCa_2Cu_{2.75}Na_{0.25}O_y$; SEM.

1. Introduction

As the resistivity of copper cables used for electricity transmission is very high, it is necessary to increase the electrical energy to very high values in order to transmit energy. To avoid the losses that can occur during transmission, transformer systems are used to increase the voltage to values such as million volts (MV) and then reduce it back to the values required by the user. The transmission of electrical energy at very high levels, such as millions of volts, and the use of many components in transmission lines both increase costs and reduce energy efficiency. These electrical conduction problems can be solved by using superconducting materials, which allow energy to be transferred without loss. By using superconductors as cables or wires in electrical transmission, DC voltage is used instead of AC voltage, eliminating the cost of voltage booster components [1]. In addition to energy transfer in technology, superconducting materials

are used for their magnetic properties in high-field magnets, high-field imaging devices in medicine, particle accelerators and magnetic sensor systems [2-5].

Enhancing the mechanical and basic superconducting properties of superconducting materials is essential to their technological application. Özkurt observed that the mechanical properties improved with the developments in the morphological structure of Bi-2212 superconducting ceramics by substituting sodium to copper oxide sites [6]. Superconducting cables with zero resistance and high current density for energy transmission must be highly resistant to external mechanical deformation when used in technological applications. Therefore, in addition to studies to improve the fundamental properties of Bi-based superconductors, studies to improve their mechanical properties are also extremely important [7-9]. Various groups have worked to enhance the mechanical characteristics of ceramic superconductors in the literature. Kurtul et al. reported that the mechanical properties of the Bi-2212 superconductor system with 0.01% Dy doping were improved due to the improvement of the crystal structure quality and the proper orientation of the superconductor grains [10]. It can be concluded that the presence of nanoparticles within the intergranular voids has a beneficial effect on the properties of the particles, resulting in enhanced mechanical and superconductivity properties. It has been reported by Akkurt et al. that the doping of Gd nanoparticles at different rates to calcium sites in the Bi-2212 superconductor system tends to weaken the mechanical properties due to the formation of distortions in the crystal structure and weak connections between the grains [11].

In our previous study, the effect of nano-sized Eu substitution on the magnetic properties in the $Bi_{1.7}Pb_{0.3}Sr_{2-x}(Eu_2O_3)_xCa_2Cu_{2.75}Na_{0.25}O_y$ (x = 0.0, 0.20, 0.25 and 0.30) system was investigated [10]. In the current study, the effect on mechanical properties of nano-sized Eu substituting on strontium sites in Bi,Pb-2223 properties was investigated. Ceramic samples generated via the solid-state reaction procedure were examined by Vickers microhardness evaluations for mechanical characteristics, Scanning Electron Microscopy (SEM) for morphological structure study, and X-ray Diffraction (XRD) for phase analysis.

2. Materials and Methods

2.1. Sample preparation

Ceramic superconductor samples in the initial composition of $Bi_{1.7}Pb_{0.3}Sr_{2-x}Eu_xCa_2Cu_{2.75}Na_{0.25}O_y$ (x = 0.0, 0.20, 0.25 and 0.30) contain high purity Bi_2O_3 (Thermo, 99%), $SrCO_3$ (Thermo, 99%), $CaCO_3$ (Thermo, 99%), CuO (Thermo, 99%), $NaCO_3$ (Thermo, 99%) and Eu_2O_3 (Nanografi, 98.5+%), 98.5+%) (80 nm) precursor powders were produced using the conventional solid state reaction method. First, an agate mortar was used to grind high-purity

precursor powders after they had been weighed into the proper amounts. Following the grinding stage, a hydraulic press machine was used to apply 375 MPa of pressure to the homogeneously mixed precursor powders, forming them into 1.5 cm diameter pellets. Following the pressing step, the pelletized samples were subjected to the first heat treatment, calcination, for 12 hours at 750 °C. To start the creation of high-purity Bi-2223 phases, the calcined pellets were ground in an agate mortar, pressed under 375 MPa pressure, and then calcined once more for 12 hours at 820 °C. Two more repetitions of the processes were carried out, which included grinding, pressing and calcination steps. To decrease crystal defects and enhance the density of high-purity Bi-2223 superconducting phases, ceramic samples needed to be annealed. The pelletized samples were milled, pressed and then annealed for 160 hours at 860 °C to apply the annealing procedure.

Ceramic samples have been identified as Sample A (x = 0.00), Sample B (x = 0.20), Sample C (x = 0.25), and Sample D (x = 0.30) based on the nano-sized Eu substitution ratio in order to provide details for the characterization procedures after the production procedure.

2.2. Characterization

A PPMS from Cryogenic Limited, which operates between 5 and 300 K and may reach cryogenic temperatures of up to 2 K in a closed-loop He system, was used to assess the samples' resistivity. An Ultima IV X-ray diffractometer from Rigaku was used to perform X-ray powder diffraction investigations in the 2θ range of 3–60° at a constant scan rate of 2°/min, in order to identify the phases comprising the samples. A Quanta FEG 650 scanning electron microscope (SEM) was used to study the surface morphologies of the samples. The average crystal size is determined using the Debye-Scherrer equation below [12, 13].

$$D_c = {\kappa\lambda}/{\beta cos\theta} \tag{1}$$

where β is the peak carry out width at half maximum (in radians) at the measured peak angle θ, λ is the X-ray wavelength (CuKα=1.5406 Å), and κ is the crystallite shape factor (0.94).

The diagonal lengths of this indentation are calculated using the formula below to calculate Vickers hardness values [13, 14].

$$Hv = 1.8544\ (P/d^2)\ GPa \tag{2}$$

The applied load, P, in Newtons, and the diameter length of the indentation, d, in micrometers, are the two variables in this equation.

The following characteristics have been calculated using the hardness values obtained from the Vickers measurements: brittleness index (B), fracture toughness (K_{IC}), yield strength (Y), and elastic modulus (E) [32]:

$$E = 81.9635Hv \tag{3}$$

$$Y \approx \frac{Hv}{3} \tag{4}$$

$$K_{IC} = \sqrt{\boldsymbol{2E\gamma}} \tag{5}$$

$$B = \frac{\boldsymbol{Hv}}{\boldsymbol{K_{IC}}} \tag{6}$$

Meyer's law is calculated with the following formula [26]

$$LogF = nLogd + LogK \tag{7}$$

3. Results and Discussion

3.1. Phase Analysis Performed by X-Ray Diffraction Measurement

X-Ray diffraction measurements performed to determine phase formations in the superconducting sample are shown in Fig. 1. In addition, the phase formations obtained by X-ray diffraction measurements of samples C and D containing nano-sized Eu at x = 0.25 and 0.30, respectively, were investigated in another study [12].

Bi-2223 phase is represented by a plus symbol (+), while the low-temperature phase of the Bi-2212, as well as the impurity phases of Ca_4PbO_3 and $Ca_4Bi_6O_{13}$, are represented by a circle (●), asterisk (⋆), and cross (■), respectively.

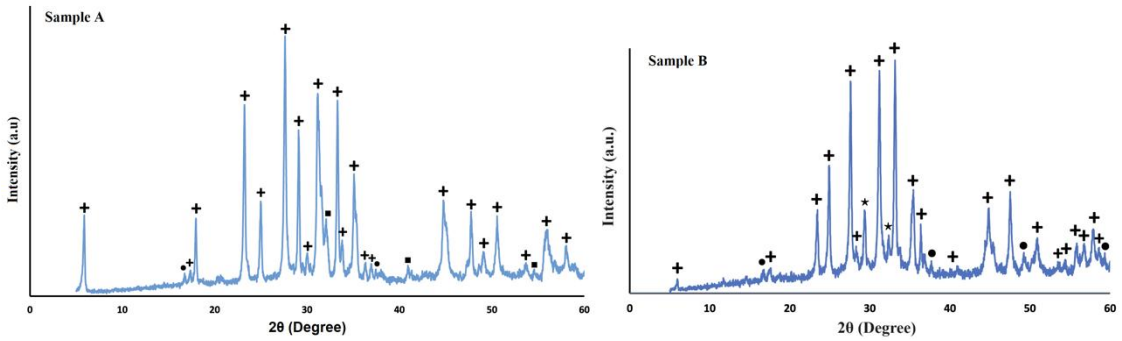


Figure 1: X-ray diffraction analysis of ceramic superconductor samples with varying ratios of nano-sized Eu substituted

While the Bi-2223 superconducting phase is the dominant phase in all samples, XRD measurements show that different impurity phases appear in samples with varying levels of nano-sized Eu substitution. Also, the formation of superconducting phases with sharp intensity and correct position in the BSCCO superconducting system may indicate that the crystallization process has occurred correctly.

The intensity and density of the characteristic peaks of the Bi-2223 phase, indicating a good crystallization process in sample A, were formed at optimal levels. In sample B containing nano-sized Eu at x = 0.20, a decrease in the intensities of the peaks belonging to the Bi-2223 phase was observed at points such as $2\theta \approx 23.0°$ and 23.1°. In addition, the impurity phases observed at points such as $2\theta \approx 32.14°$ and 40.64° in sample A were not observed in sample B. An improvement in electrical characteristics can be assumed in Sample B since the impurity phases' disappearance at certain points can raise the system's phase stability. However, the impurity phases increased and the intensity of the peaks corresponding to the superconducting phases decreased as the nano-sized Eu substituting ($x > 0.25$) increased [10].

The lattice parameter values of the samples are given in Table 1. Examining the lattice parameter values of the ceramic superconductor samples in the table, it can be seen that they are compatible with the Bi-2223 superconductor phase with the tetragonal crystal structure in the literature [16, 17].

Table 1: Crystal structure parameters of ceramic samples

Sample	T (K)	a (Å)	b (Å)	c (Å)	Crystal Size (nm)
Sample A	80.073	5.369	5.369	36.943	32.11
Sample B	90.089	5.396	5.396	37.632	23.45
Sample C	70.106	5.401	5.401	37.545	24.89
Sample D	-	5.407	5.407	36.892	25.91

The crystal size calculated by the Debye-Scherrer method is presented in Table 1. As can be seen from the values in the table, an increase in crystal size occurred with the introduction of nano-sized Eu particles into the structure. It is a known effect in the literature that when nano-sized particles are substituted into the BSCCO ceramic superconductor, they settle between the superconductor grains and increase the grain size [18, 19]. Increasing the grain size within the crystal structure of ceramic superconductor samples can increase their current carrying capability. However, increasing the size of the grains can result in gaps and high angles between the grains. This situation can affect properties based on intergranular performance, such as mechanical properties, by compromising the homogeneity of the morphological structure.

3.2. Morphological Analyses with Scanning Electron Microscope Measurements

Figure 2 shows the results of the scanning electron microscope measurement, which was used to investigate the ceramic samples' morphological structure.

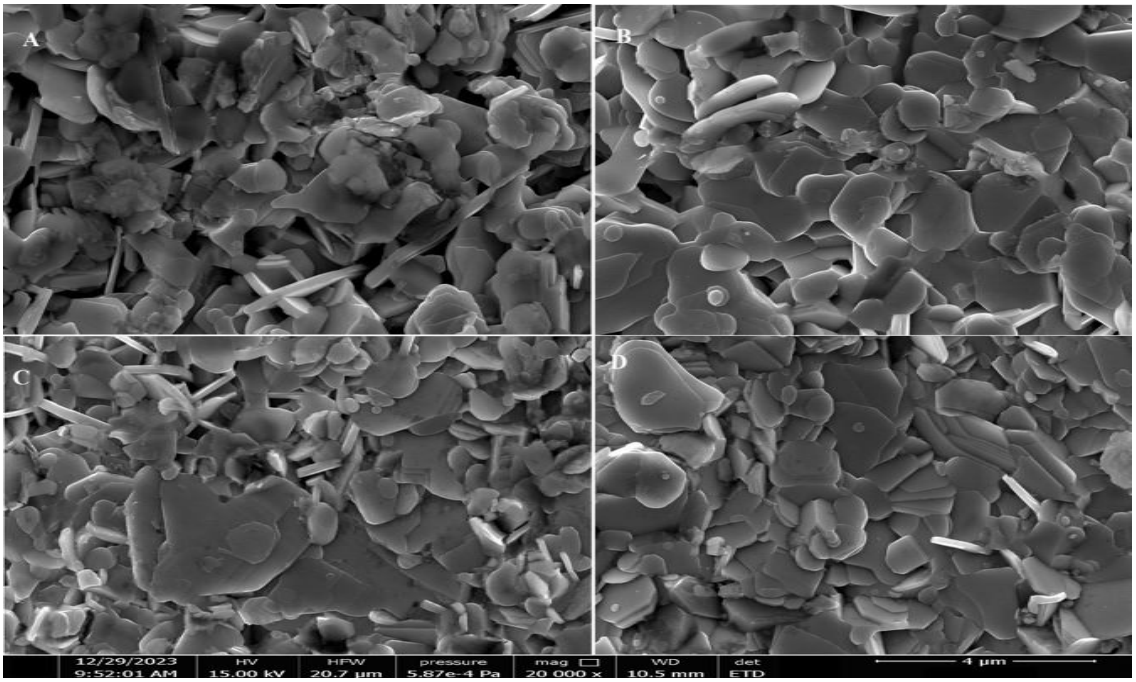


Figure 2: Morphologic results of the (A) sample A, (B) sample B, (C) sample C (D) sample D

The distribution of different grain types in various orientations within the samples can be seen as a sign that a polycrystalline structure is forming. It is well known that flaky plate-like grain structures indicate the presence of Bi-2223 superconducting phase structure, while plate-like grains can explain the formation of Bi-2212 superconducting phase structure [20, 21]. All samples' surfaces showed an appearance of flaky plate-like grain structures in addition to plate-like grain structures, which is consistent with the XRD data. This suggests that Bi-2223 phases were mostly formed together with the presence of Bi-2212 superconducting phases.

In sample A, which does not contain Eu at nano-sized, the formation of large-sized grains, which are affected by the sodium element in the morphological structure, is observed. However, porous structures between large grains occurred in sample A. In addition, in the sample containing x = 0.20 nano-sized Eu, the voids between the grains decrease and the grains are more regular oriented. In ceramic superconductor samples, the morphological structure is evolved by the regular orientation and strong bonding of the superconductor grains. Such developments have significant effects on mechanical properties as well as having positive effects on electrical and magnetic properties. On the other hand, the formation of strong intergranular bonding and low-level porosity structure affects the development of mechanical properties in ceramic

superconductor materials [22, 23]. Dogruer et al. reported that mechanical properties of Bi-2212 superconductor samples weakened with increasing Cr doping due to weak intergrain connections, porous structure formation, irregular orientation of grains and impurity phase formation [24]. The morphological structure of sample C shows a distribution of grains of different sizes, a less porous structure and a smooth alignment between the grains. Khalil reported improvement in mechanical properties in the $Bi_2Sr_2Ca_{1-x}Y_xCu_2O_{8+\delta}$ system due to the 0.35 Y doping improving the superconducting intergranular connections [25]. In sample D, although the grains had a regular orientation, wide angles between the grains were observed in some regions. substitution of Eu at the nanoscale led to the strengthening of the intergranular bonds. The mechanical development observed in the literature relating to these morphological effects may also occur in samples containing nano-sized Eu.

On the other hand, Table 1 also displays the ceramic samples' onset transition temperature values (T_c^{onset}). Due to phase structural changes and the creation of strong bonds between the superconducting grains, the sample that was substituted with nano-sized Eu at x = 0.20 showed the highest superconductivity transition temperature. In the sample containing nano-sized Eu at x= 0.30, superconductivity transition could not be observed due to the impurity phases forming a barrier between the superconducting phases and the increase in the density of crystal defects.

3.3. Characterization of Mechanical Properties of Ceramic Samples

The brittle structure of high-temperature superconductors, due to their ceramic nature, is an important problem that needs to be solved in order to use them as cables in technological applications. Dislocations in the crystal structure, porosity and microcracks are the factors that affect the mechanical strength and elastic properties of high-temperature superconductors [26]. Mechanical measurements that provide information about the strength and deformation of superconducting materials are extremely important. Vickers microhardness is a widely used technique in the mechanical analysis of ceramic materials such as BSCCO superconductors [27, 28].

Figure 3 shows the graph of hardness used to describe the mechanical properties of ceramic superconductor samples.

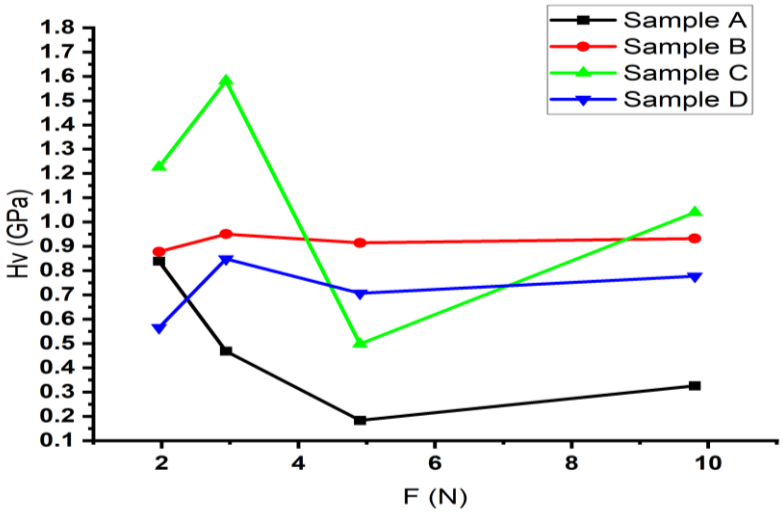


Figure 3: Vickers microhardness measurement results of samples A, B, C and D

Bi-based high-temperature superconductors consist of randomly distributed plate-like grains with a porous structure between the grains. Irregular positioning and void structure can weaken inter-granular bonding and cause wide angles to form between grains. The development of mechanical properties depends on the solution of these problems. Especially nano-sized particles that can be placed between the grains can be a solution to this problem. Therefore, the improvement of the mechanical properties of these superconductors depends on factors such as improving the porous structures and weak intergranular connections in their microstructures [29, 30]. The formation of voids between grains in the morphological structure of Sample A is explained. In Sample A, due to the formation of the irregular grain structure, the mechanical properties were weakened by the achievement of low Hv values. Moreover, the decrease in the porous structure occurred due to the settlement of nano-sized Eu particles between the grains. Due to the reduction of the porous structure, the connections between the superconductor grains can be strengthened. With the increase in nano-sized Eu substituting, the hardness value increased, indicating that the mechanical properties improved due to the developments in the morphological structure. Compared to the other samples, the highest hardness value at maximum load was obtained in the sample with x = 0.25 nano-sized Eu substitution.

Parameters such as young modulus, yield strength, fracture toughness and brittleness index are presented in Table 2. The behavior of all parameters calculated in Table 2 is consistent with the actual Hv behavior obtained by Vickers microhardness measurement. Both the size of the crystal and the development of strong links between the superconducting grains can be affected by the smooth grain formation in the morphological structure [31]. In the Sample C, the hardness value increased with the improvements in the morphological structure and crystal

properties. This has also led to the improvement of theoretically calculated parameters such as Young's modulus, yield strength, fracture toughness and brittleness index.

Table 2: The ceramic samples' load-dependent Hv, E, Y, K_{IC}, and B values were replaced with nano-sized Eu

Samples	F (N)	d (um)	Hv (GPa)	E (GPa)	Y (GPa)	K_{IC}	B
Sample A	1.96	66.5	0.838	68.740	0.279	0.346	2.418
	2.94	109	0.468	38.378	0.156	0.259	1.806
	4.9	225	0.183	15.011	0.061	0.162	1.130
	9.8	276.25	0.325	26.695	0.108	0.216	1.507
Sample B	1.96	65	0.877	71.949	0.292	0.354	2.474
	2.94	76.5	0.950	77.915	0.316	0.369	2.574
	4.9	126	0.914	74.932	0.304	0.362	2.524
	9.8	167.5	0.932	76.423	0.310	0.365	2.549
Sample C	1.96	55	0.877	71.949	0.292	0.354	2.474
	2.94	63.5	0.950	77.915	0.316	0.369	2.574
	4.9	136.5	0.914	74.932	0.304	0.362	2.524
	9.8	141	0.932	76.423	0.310	0.365	2.549
Sample D	1.96	81	0.122	10.049	0.040	0.132	0.924
	2.94	98.5	0.158	12.964	0.052	0.150	1.050
	4.9	195	0.497	40.787	0.165	0.267	1.862
	9.8	212.5	0.103	8.5218	0.034	0.122	0.851

Approaches and models such as Meyer's law, which are empirical and semi-empirical equations, have been proposed to describe the variation of indentation size with the applied test load. Meyer's law is the simplest method of interpreting the ISE or RISE behavior of samples.

According to Meyer's law, when the n value is less than 2, the behavior called ISE is exhibited, where the hardness values decrease with increasing load values, while when the n value is greater than 2, the behavior called RISE is exhibited, where the microhardness values increase with increasing load values [33, 34]. The parameters in Eqn. (7) were found from the Ln(d) and Ln(F) graphs given in Fig. 4. The hardness parameters from Meyer's law are presented in Table 3.

Table 3: Hardness analysis of all samples according to Meyer's Law

Samples	n	*K* (GPa)
Sample A	1.009	0.033
Sample B	1.558	0.003
Sample C	1.278	0.017
Sample D	1.344	0.007

The n value was calculated from the slope of the graph in Fig. 4. In the graph, linear behavior is exhibited in all examples and the n value is less than 2. All examples exhibit ISE ($n<2$)

behavior. The ISE behavior obtained by Meyer's law is the general behavior in the BSCCO superconductor system [27, 28]. The results obtained in Fig. 3 are in good agreement with the micro hardness measurement results.

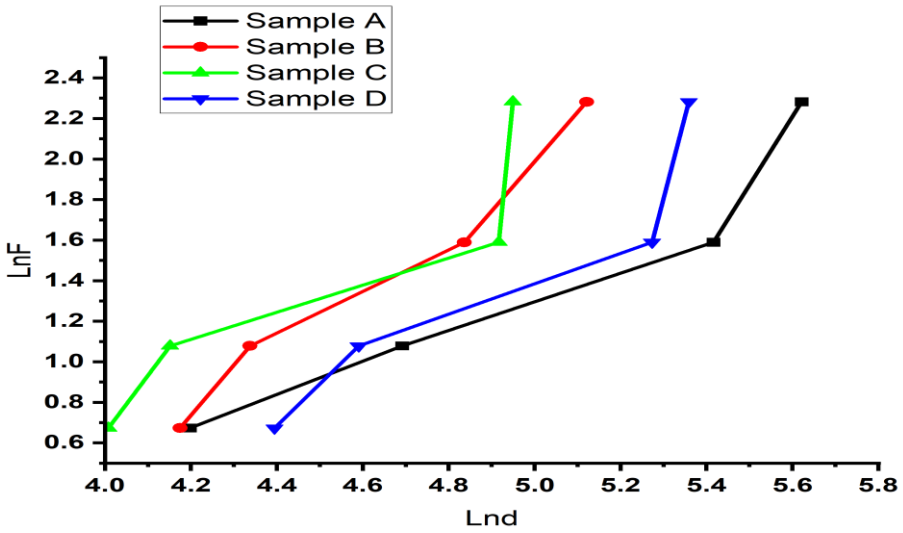


Figure 4: Applied load LnF and diagonal Lnd plot of Samples A, B, C and D

4. Conclusion

In the present work, the mechanical properties of ceramic superconductors with the initial composition $Bi_{1.7}Pb_{0.3}Sr_{2-x}(Eu_2O_3)_xCa_2Cu_{2.75}Na_{0.25}O_y$ (x = 0.00, 0.20, 0.25 and 0.30) were investigated. The brittle nature of cuprate superconductors, due to their ceramic nature, limits research into their mechanical properties. The most common method for characterizing the mechanical properties of superconductors in ceramic structures is the Vickers microhardness measurement method. To investigate the morphological and mechanical properties of samples containing different proportions of Eu nanoparticles, XRD, SEM and Vickers microhardness measurements were carried out, respectively. In the phase structure analyses, despite the formation of some minor secondary phases in all samples, the main phase structure was identified as being the Bi-2223 phase. In accordance with the results of the phase analysis, it turned out that all of the samples' morphological structures included grain structures that belonged to the Bi-2223 phase. With increasing nano-sized Eu substituting, a decrease in the porous structure occurred in the samples. With the improvements in the morphological structure, the best mechanical properties were obtained in the sample containing nano-sized Eu at x = 0.25 with a hardness value of 100.04 GPa under 9.8 N load. In addition, mechanical characterization was expanded by applying different methods between the applied test load and microhardness value. ISE behavior, which is the general behavior of BSCCO ceramics, was detected in the samples.

Acknowledgements

All samples were prepared in the Nanomaterials/Magnetic Materials Research Laboratory (NM_3RLab) Adana Alparslan Türkeş Science and Technology University in Türkiye. SEM and XRD measurements were carried out in Çukurova University Central Research Laboratory (ÇÜMERLAB) in Turkey. Vickers microhardness measurement was carried out in Tarsus University.

Funding Information

This study is supported by TUBITAK with project number 122C061 within the scope of "2218 - National Postdoctoral Research Fellowship Program".

References

[1] Aytekin, M.E., Akyol, M., Özkurt, B., *Improvement in electrical properties of Bi-2212 superconducting materials substituted with large-scale nano-sized tin*, Applied Physics A, 130, 68–78, 2024.

[2] Shen, T., Garcia Fajardo, L., *Superconducting accelerator magnets based on high-temperature superconducting Bi-2212 round wires,* Instruments, 4(2), 17– 39, 2020.

[3] Yin, S., Swanson, J., Shen, T., *Design of a high toughness epoxy for superconducting magnets and its key properties,* IEEE Transactions on Applied Superconductivity, 30, 1–5, 2020.

[4] Chen, P., Trociewitz, U.P., Dalban-Canassy, M., Jiang, J., Hellstrom, E.E., Larbalestier, D.C., *Performance of titanium oxide–polymer insulation in superconducting coils made of Bi-2212/Ag-alloy round wire,* Superconductor Science and Technology, 26, 075009, 2013.

[5] Al Azzawi, A.N.S., Türköz, M.B., Erdem, Ü., Yildirim, G., *Improvement in organization of Cu–O coordination and super-electrons in Bi-2212 ceramic matrix with Ag/Sr partial substitution*, Journal of Materials Science: Materials in Electronics, 35, 1236–1261, 2024.

[6] Özkurt, B., *The influence of Na addition on the mechanical properties of Bi-2212 superconductors*, Journal of Superconductivity and Novel Magnetism, 27, 2407–2414, 2014.

[7] Aytekin, M.E., Özkurt, B., Sugözü, İ., *Physical, magnetic and mechanical properties of Bi-2212 superconductors prepared by high pelletization pressure*, Journal of Materials Science: Materials in Electronics, 26, 1799–1805, 2015.

[8] Zalaoglu, Y., Turgay, T., Ulgen, A., Erdem, U., Turkoz, M., Yildirim, G., *A novel research on the subject of the load-independent microhardness performances of Sr/Ti partial displacement in Bi-2212 ceramics*, Journal of Materials Science: Materials in Electronics, 31, 22239–22251, 2020.

[9] Kahraman, F., *Evaluation of the Vickers microhardness and fracture toughness on hot pressed Bi-2212/Ag ceramic composites*, Journal of Materials Science: Materials in Electronics, 27, 8006–8012, 2016.

[10] Kurtul, G., Ulgen, A.T., Armagan, O., Turkoz, M. B., Erdem, Ü., Yildirim, G., *Role of dysprosium substitution on microscopy architecture, structural stability, and crack propagation mechanism in Bi-2212 engineering ceramics*, Physica Scripta, 100(2), 025932, 2025.

[11] Akkurt, B., Yildirim, G., *Change of mechanical performance and characterization with replacement of Ca by Gd nanoparticles in Bi-2212 system and suppression of durable tetragonal phase by Gd,* Journal of Materials Science: Materials in Electronics, 27(12), 13034–13043, 2016.

[12] Aytekin, M.E., Akyol, M., *Effect of Nano-Sized Europium Substitution on Strontium Sites on Diamagnetic Properties in BiPb-2223 Superconductor System*, Journal of NanoScience in Advanced Materials, 3(1), 8–14, 2024.

[13] Fallah-Arani, H., Sedghi, A., Baghshahi, S., Moakhar, R. S., Riahi-Noori, N., Nodoushan, N.J., *Bi-2223 superconductor ceramics added with cubic-shaped TiO_2 nanoparticles: Structural, microstructural, magnetic, and vortex pinning studies*, Journal of Alloys and Compounds, 900, 163201, 2022.

[14] Saxena, R.B., Giri, R., Awana, V.P.S., Singh, H.K., Ansari, M.A., Kumaraswamy, B.V., et. al., *Impact of zn Substitution on Phase Formation and Superconductivity of $Bi_{1.6}Pb_{0.4}Sr_2Ca_2Cu_{3-x}Zn_xO_{10-\delta}$ with x= 0.0, 0.015, 0.03, 0.06, 0.09 and 0.12,* Modern Physics Letters B, 19, 771–778, 2005.

[15] Yıldız, A., Kocabaş, K., Akyüz, G.B., *Dependence of the Structural, Electrical and Magnetic Properties of $YBa_2Cu_3O_{7-\delta}$ Bulk Superconductor on the Ag Doping*, Journal of superconductivity and novel magnetism, 25, 1459–1467, 2012.

[16] Kır, M.E., Özkurt, B., Aytekin, M.E., *The effect of K-na co-doping on the formation and particle size of Bi-2212 phase*, Physica B: Condensed Matter, 490, 79–85, 2016.

[17] Saghafi, M., Shams, G., Soltani, Z., *The influence of Sm_2O_3 nanoparticles adding on some superconducting properties of $Bi_{1.6}Pb_{0.4}Sr_2Ca_2Cu_3O_{10+\delta}$ ceramics*, Physica C: Superconductivity and its Applications, 624, 1354566, 2024.

[18] Aytekin, M.E., *Change in Physical, Electrical and Magnetic Properties of Bi-2212 Superconducting Materials Co-Substituted with Nano-Sized Zinc and Sodium*, Transactions on Electrical and Electronic Materials, 25, 779–791, 2024.

[19] Arlina, A., Halim, S., Kechik, M.A., Chen, S., *Superconductivity in Bi–Pb–Sr–Ca–Cu–O ceramics with YBCO as additive,* Journal of Alloys and Compounds, 645, 269–273, 2015.

[20] Fallah-Arani, H., Koohani, H., Tehrani, F.S., Noori, N.R., Nodoushan, N.J., *The structural, magnetic, and pinning features of Bi-2223 superconductors: Effects of SiC nanoparticles addition,* Ceramics International, 48, 31121–31128, 2022.

[21] El Makdah, M.H., El Ghouch, N., El-Dakdouki, M.H., Awad, R., Matar, M., *Synthesis, characterization, and Vickers microhardness for $(YIG)_x$/(Bi, Pb)-2223 superconducting phase*, Ceramics International, 49, 22400–22422, 2023.

[22] Ozturk, O., Arebat, R.A.M., Nefrow, A.R.A., Bulut, F., Guducu, G., Asikuzun, E., et. al., *Investigation of structural, superconducting and mechanical properties of Co/Cu substituted YBCO-358 ceramic composites,* Journal of Materials Science: Materials in Electronics, 30(8), 7400–7409, 2019.

[23] Khalil, S. M., *Enhancement of superconducting and mechanical properties in BSCCO with Pb additions*, Journal of physics and chemistry of solids, 62(3), 457–466, 2001.

[24] Dogruer, M., Yildirim, G., Ozturk, O., Belenli, I., Terzioglu, C., *Variation of mechanical properties of Cr doped Bi-2212 superconductors*, Journal of Superconductivity and Novel Magnetism, 26(9), 2949–2954, 2013.

[25] Sedky, A., and Al-Battat, W., *Effect of Y substitution at Ca site on structural and superconducting properties of Bi: 2212 superconductor*, Physica B: Condensed Matter, 410, 227–232, 2013.

[26] Saritekin, N., Üzümcü, A., *Improving superconductivity, microstructure, and mechanical properties by substituting different ionic Pb elements to Bi and Ca elements in Bi-2223 superconductors*, Journal of Superconductivity and Novel Magnetism, 35, 2259–2273, 2022.

[27] Kölemen U., Uzun, O., Yılmazlar, M., Güçlü, N., Yanmaz, E., *Hardness and microstructural analysis of $Bi_{1.6}Pb_{0.4}Sr_2Ca_{2-x}Sm_xCu_3O_y$ polycrystalline superconductors*, Journal of Alloys and Compounds, 415, 300–306, 2006.

[28] Safran, S., Kılıç, A., Kılıçarslan, E., Ozturk, H., Alp, M., Asikuzun, E., et. al., *Mechanical, microstructural and magnetic properties of the bulk BSCCO superconductor prepared by two different methods*, Journal of Materials Science: Materials in Electronics, 26, 2622–2628, 2015.

[29] Khalil, S., *Enhancement of superconducting and mechanical properties in BSCCO with Pb additions,* Journal of Physics and Chemistry of Solids, 62, 457–466, 2001.

[30] Sarıtekin, N.K., Bilge, H., Kahraman, M.F., Zalaoğlu, Y., Pakdil, M., Doğruer, M., et. al., *Improvement of mechanical characteristics and performances with Ni diffusion mechanism throughout Bi-2223 superconducting matrix*, AIP Conference Proceedings, 1722, 2016.

[31] Dogruer, M., Zalaoglu, Y., Yildirim, G., Varilci, A., Terzioglu, C., *Effect of diffusion-annealing time ($0.5\ h \leq t \leq 2\ h$) on the mechanical and superconducting properties of Cu-diffused bulk MgB_2 superconductors by use of experimental and different theoretical models*, Journal of Materials Science: Materials in Electronics, 24, 2019–2026, 2013.

[32] Awad, R., Abou Aly, A. I., Kamal, M., Anas, M., *Mechanical properties of $(Cu_{0.5}Tl_{0.5})$-1223 substituted by Pr*, Journal of superconductivity and novel magnetism, 24, 1947–1956, 2011.

[33] Ozturk, O., Cetinkara, H. A., Asikuzun, E., Akdogan, M., Yilmazlar, M., and Terzioglu, C., *Investigation of mechanical and superconducting properties of iron diffusion-doped Bi-2223 superconductors*, Journal of Materials Science: Materials in Electronics, 22, 1501–1508, 2011.

[34] Özkurt, B., *The mechanical properties of Y-doped Bi-2223 superconductors*, Journal of Superconductivity and Novel Magnetism, 26, 261–266, 2013.